Deliverable D 4.2
Thermomechanical characterization of refractory materials finished

Document type	**Deliverable D 4.2**
Document Version / Status	**1.30**
Primary Authors	**Marc Huger, marc.huger@unilim.fr, UNILIM**
Distribution Level	**PU (Public)**
Project Acronym	**ATHOR**
Project Title	**Advanced THermomechanical multiscale mOdelling of Refractory linings**
Grant Agreement Number	**764987**
Project Website	**www.etn-athor.eu**
Project Coordinator	**Marc Huger, marc.huger@unilim.fr, UNILIM**
Document Contributors	**Marc Huger, marc.huger@unilim.fr, UNILIM** **Rafael Oliveira, rafael.oliveira@uc.pt, UMINHO** **Robert Kaczmarek, robert.kaczmarek@unilim.fr, UNILIM**

History of Changes

Version	Date	Author (Organization)	Change	Page
1.0	01/07/2020	Rafael Oliveira (UMINHO) Robert Kaczmarek (UNILIM)	First version created	All
1.1	03/07/2020	Glyn Derrick (UNILIM)	Formatting and English check	All
1.2	07/07/2020	Robert Kaczmarek (UNILIM)	Minor corrections	2, 3, 7, 9
1.30	03/10/2020	Marc Huger (UNILIM)	Proof reading	All

Table 1. Related Work Packages status

Work package	Task	Description
WP4 - Advanced measurements for numerical validation	Task 4.2 - Quantification of the thermal gradient effect on materials	The objective is here to characterize the refractory materials at a sample scale (brick) under cyclic thermal gradient.

TABLE OF CONTENTS

1 Introduction

This report will review the thermomechanical behaviour of refractory materials at a sample scale (brick) under cyclic thermal gradient. A dedicated device has been previously developed in a very first version, in the framework of another European program (SFERA2), to monitor (only by acoustic emission for this first version) the behaviour of a cylindrical disc (10 to 15 cm in diameter) subjected to a concentrated heat flux (from a solar concentrator) on top surface of the sample. The focus of the work done in the framework of the present European program ATHOR (and reported within the present deliverable), was to developpe a second version of this device named ATHORNA for Advanced measurements for in-situ Thermomechanical monitORing of large sample uNder thermal gradient. For this second version of the device, the three main axes of development were to use a CO_2 laser as heat source (for more flexibility on imposed thermal cycles), and to use an optimal combination of 2 optical cameras with an infrared camera in order to measure the evolution of strain/temperature maps through all the back surface of the disk. In line with the global purpose of the present WP4 (dedicated to advanced measurements for numerical validation), these strain and temperature measurements have been compared to numerical FEM model (WP3) based on materials properties provided by WP2. As a preliminary stage, results are presented here with a specific focus on alumina-spinel bricks used in steel ladles at TataSteel plant in IJmuiden.

2 Experimental methods

2.1 GENERAL DESCRIPTION OF THE DEVICE

2.1.1 Sample preparation

The thermal shock test presented in this deliverable is performed on fired alumina spinel refractory material [1]. The sample has disk shape with thickness of 10 mm and diameter of 100 mm. The bottom of the sample is covered with painted black and white speckle pattern, in order to monitor deformation of sample surface using digital image correlation (see Figure 1a).

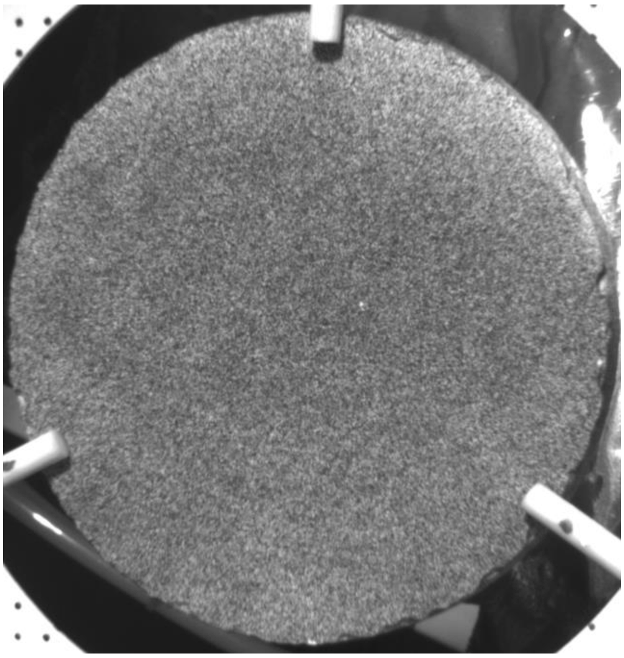

(a)

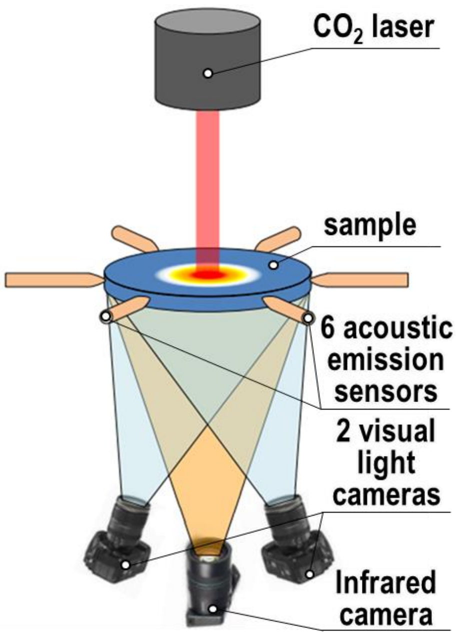

(b)

Figure 1: a) Speckle pattern made of black and white paints; b) Schema of ATHORNA device.

2.1.2 Applied laser program

The characterization of refractory materials under a cyclic thermal gradient is performed using the ATHORNA device (see Figure 1b). Cyclic thermal gradients are induced within the sample by irradiation of the sample's top surface by a CO_2 laser beam. The arriving beam (diameter **16** mm) heats the centre of the sample's top surface, inducing a hot thermal shock. The applied laser cycles have a constant power and an increasing irradiation time (see Figure 2): from 0.5 s, at the first cycle to 6 s at the 12^{th} cycle, with a duration increase of 0.5 s per cycle.

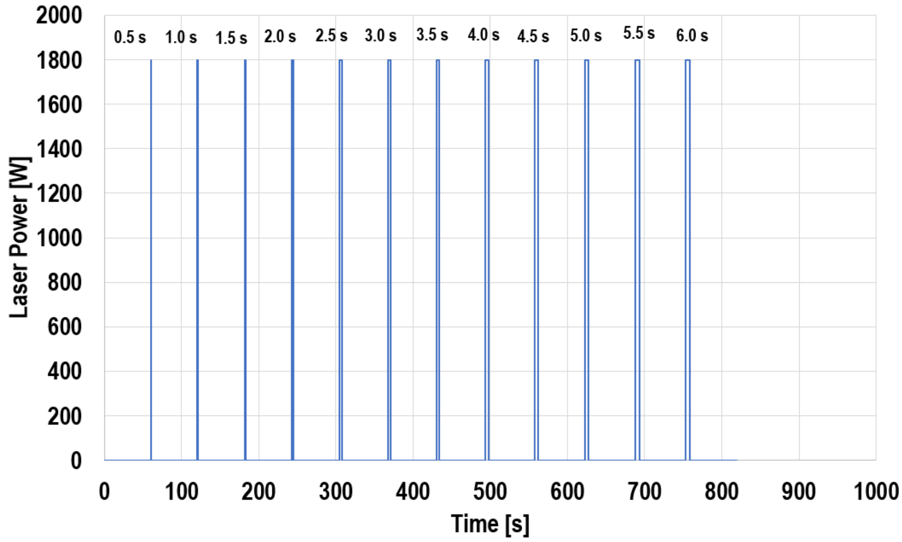

Figure 2: Laser cycles applied to the alumina spinel sample.

2.1.3 Monitoring of sample behaviour

The sample's response was monitored by the recording of the bottom surface, using thermal and visual sensors (acoustic emissions sensors were not used during this test). Output data allows the analysis of 2D temperature field and 3D strain field during the entire test. With the application of a stereoscopic vision system (synchronized image acquisition from the 2 optical cameras with precisely determined position and orientation), coupled with the Digital Image Correlation (DIC) technique, this ATHORNA device allows the measurement of both in-plane and out-of-plane displacements. The 2P-DIC (Two Parts Digital Image Correlation) technique [2], being specially designed for monitoring of fracture behaviour, can be used to detect emerging material discontinuities and highlight them on images, as well as to determine crack length evolution through the overall thermal shock test. For estimation of crack initiation time at very early stage, the crack opening value has been measured using standard DIC method in the vicinity of the very starting point of the crack observed by 2P-DIC. In fact, using two small subsets (in this case 32x32 pix.^{2}) with distance between their centres of about 70 pix. (magnification of 0.079 mm/pix.) located on both sides of the starting point of the crack (observed later by 2P-DIC) gives a more accurate crack initiation time since significant small strain increase can be observed just before robust detection by 2P-DIC algorithm.

2.2 AUXILIARY NUMERICAL MODELLING

An auxiliary numerical model was developed using the software ABAQUS [3]. This software has been successfully used in other studies to simulate refractory materials at room and elevated temperatures [4], [5]. The goal of the numerical model is to complement the experimental campaign and assess the stresses fields developed in the sample and the temperatures in the hot face.

2.2.1 Material modelling

The material was modelled with a temperature-dependent plastic behaviour. As input for FEM modelling (WP3), the thermo-mechanical properties (from WP2) are presented in Table 1. The emissivity of the alumina spinel was taken at 0.80 for the surfaces free of painting and at 1.0 for the painted surface (bottom face). The convection coefficient was taken as 12 W/(m^2.°C).

Table 1: Thermal and mechanical properties of alumina-spinel material with a density of 3130 kg/m^3

Temperature (ºC)	Young Modulus (GPa)	Specific Heat (J/kgºC)	Thermal Elongation	Thermal conductivity (W/mºC)
20	28.77	805	0.00%	6.426
200	27.89	1073	0.12%	4.86
400	28.60	1161	0.28%	3.789
600	29.32	1221	0.46%	3.12
800	31.27	1263	0.63%	2.942
1000	34.52	1293	0.82%	2.656
1200	34.71	1318	1.02%	2.408
1300	34.37	1330	1.12%	2.398

The sample was irradiated at the top surface by a CO_2 laser beam with pre-defined cycles. The laser was concentric with the centre of the sample. The distribution of the heat flux on the specimen's surface is defined by an analytical equation as shown in Eq. 1, where I_o is the maximum heat flux applied, x and y are coordinates of a cartesian system located at the centre of the sample, and w is the waist of the laser (taken as 8 mm), corresponding to the radius for which the intensity decreases by the factor of $1/e^2 = 0.135$. The total power applied to the sample is defined by Eq. 2.

$$I(x,y) = I_O \times e^{-\frac{2(x^2+y^2)}{w^2}} \quad \textit{Eq. 1}$$

$$Power = \iint I(x,y) \quad \textit{Eq. 2}$$

2.2.2 Mesh and element type

The specimen was modelled using solid elements C3D8R, defined as a continuum three-dimensional hexahedral and eight-node brick with reduced integration, this element has hourglass control and linear interpolation. It was observed that good results could be obtained by using finite elements of approximately 0.75x0.75x0.75 mm.

2.2.3 Analysis procedure

A coupled temperature-displacement analysis was performed. The heat transfer and the mechanical analysis are performed simultaneously, the outputs of the analysis are the fields of temperature, displacements, strains and stresses. The total time of analysis was 820 s. The maximum increment of time was taken as 0.5 seconds and the maximum allowable temperature change per increment was 25 ºC.

3 Results

This section presents the experimental results of the tests performed on the ATHORNA device. The experimentally measured temperatures, strains and displacements are being compared to the predictions of the numerical model. In order to facilitate the visualisation of the results, the comparison is focused on three key points from the cold face of the sample: a) P1: centre; b) P2: mid-radius; c) P3: close to the border (5 mm from the border), see Figure 3. The out-of-plane displacements were validated only for P1, as the thermal bowing presents significant values only in the centre of the sample.

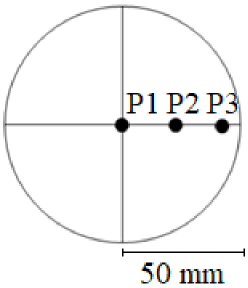

Figure 3: Key points from the cold face of the sample used for comparison between modelled and experimental values of temperatures and strains.

3.1 TEMPERATURE FIELD

Figure 4 (a) shows the evolution of the temperature versus time in the centre (P1) of the alumina spinel disc. The temperatures experimentally measured by the infrared camera and the temperatures predicted by the numerical model at the cold face are in good agreement. Figure 4 (b), (c) and (d) show the temperatures along the diameter of the sample by the end of 3rd, 6th and 9th laser cycles.

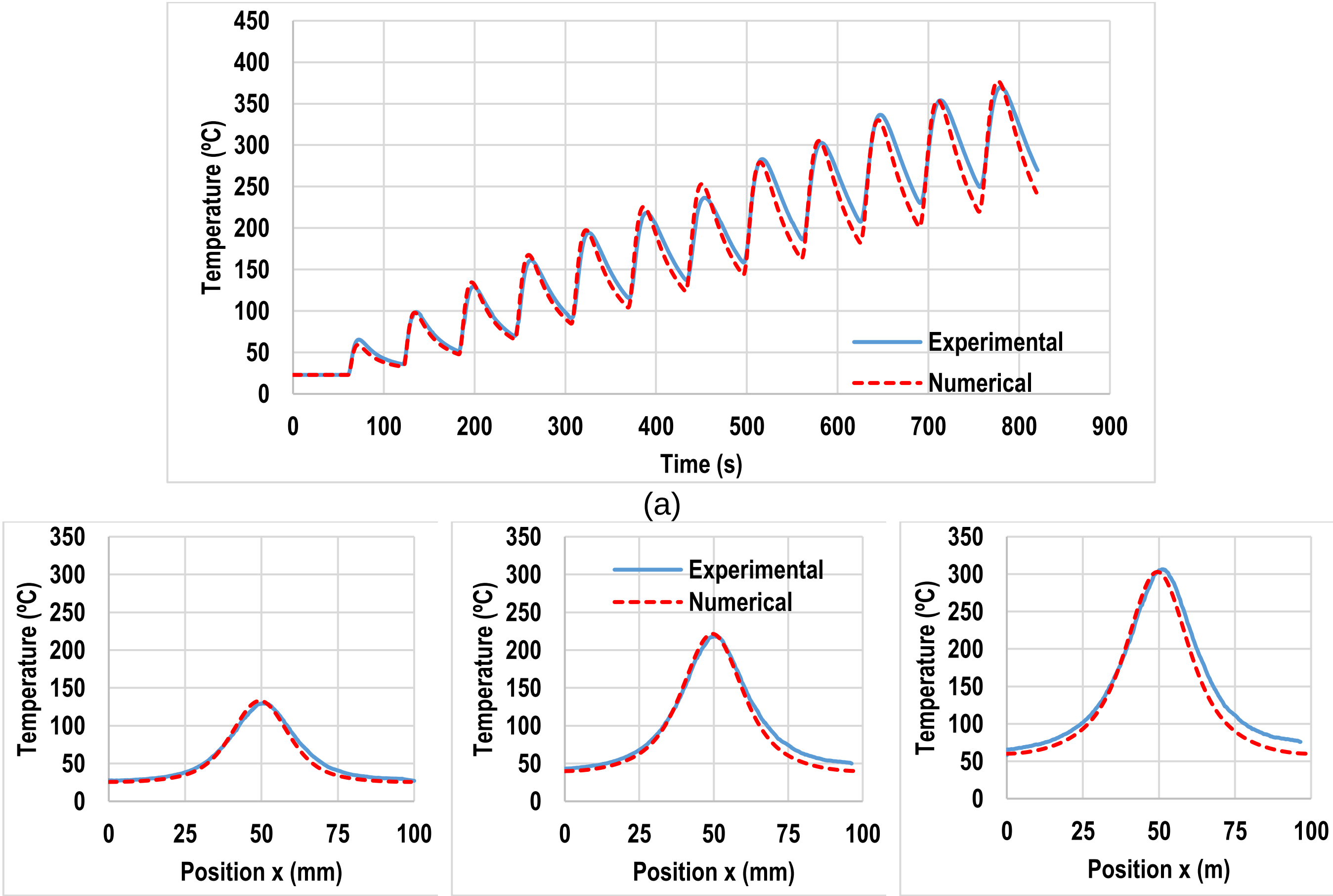

Figure 4: Temperature evaluation on considered alumina spinel sample: a) temperature at point P1 versus time; b) temperatures along diameter for 3rd cycle; c) temperatures along diameter for 6th cycle; d) temperatures along diameter for 9th cycle

The experimentally measured thermal gradient between P1 and P2, and between P1 and P3 are 201 ºC and 230 ºC, respectively, both at the end of the last laser cycle. The maximum temperature gradient between the hot face and the cold face predicted by the numerical model is 3208 ºC, obtained at the end of the 8th laser cycles, as shown in Figure 5. Even if no measurement can confirm this huge temperature gradient in the very central part of the disk, one can easily observe that an area of a couple of mm in diameter has been fused in the middle of top surface of the treated disk (knowing that melting points of Alumina and Spinel are 2070°C and 2135°C respectively).

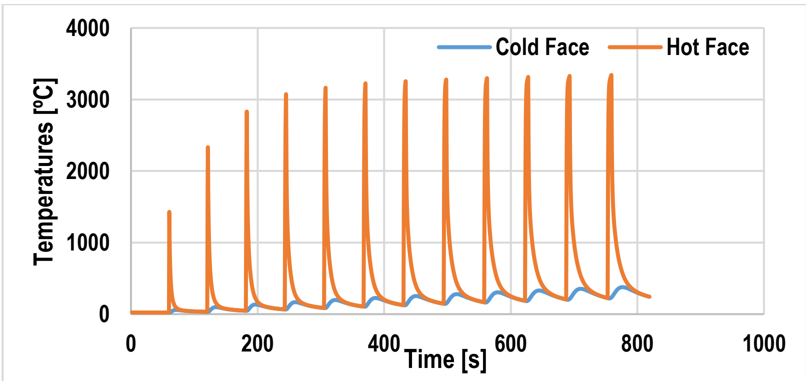

Figure 5: Predicted thermal gradient between the hot and cold faces in the very central part of the disk.

There are two thermal gradients within the sample: *i*) through the thickness of the disk and *ii*) between the centre and the borders. The thermal gradient though the thickness of the disk leads to a thermal bowing, as the temperatures in the centre of the top face are significantly higher than the temperatures in the centre of the bottom face. The temperature gradient between the centre and the borders of the sample leads to compressive stresses in the radial direction. In the circumferential direction it leads to compressive stresses in the centre of the sample and tensile stresses at the borders. The successive cycles with increasing time lead to thermal shocks with an increasing level of stresses. Thus, when the tensile stresses in the border of the disk reaches the tensile strength of the investigated material, cracks can occur with a starting point at the border. In order to illustrate this point, strain levels developed through the bottom face of the disk are being presented in the next section.

3.2 STRAIN FIELD

Figure 6 presents the strains measured by digital image correlation (at the bottom of the sample's surface, with X and Y correspond to coordinates on this surface) and the strains predicted by the FEM numerical model for the investigated alumina spinel refractory disk. In spite of the heterogeneous microstructure of the alumina spinel material, a reasonable correlation was found between the experimental and numerical values. Exp.E_{xx}, Exp.E_{yy} and Exp.E_{xy} stand for experimental measured strains in directions X, Y and XY (shear), respectively. The numerical predicted strain is denoted by Num. E_{xx} / E_{xx} (exactly similar in two perpendicular direction with FEM modelling). The developed model reproduces the heating and cooling of the sample with good accuracy. The maximum strain measured by the DIC technique was 0.0026 and the maximum strain predicted by the numerical model was 0.0020.

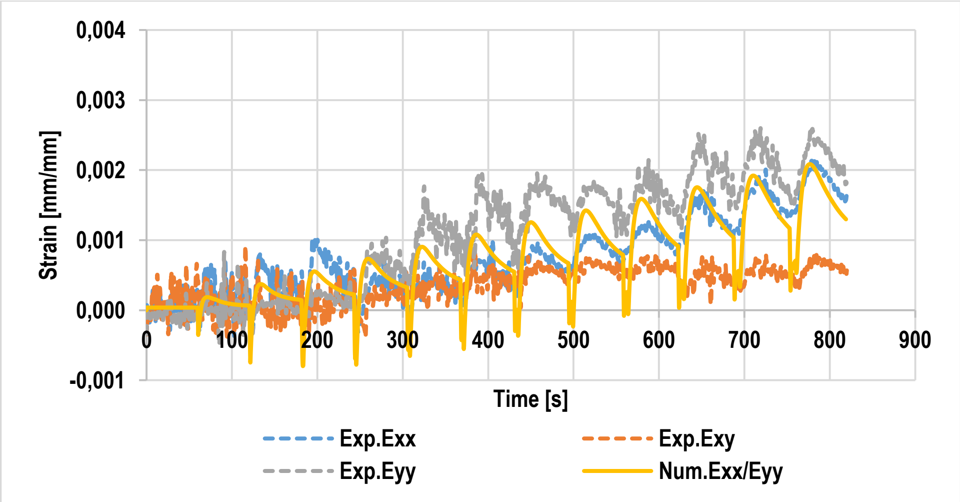

Figure 6: Strains developed in the alumina spinel sample at point P1

The digital image correlation allows the determination of the total strains components (ε_{total}). It is possible to determine the thermal strains (ε_{therm}) based on the measurements of the IR camera. Therefore, it is possible to determine the mechanical strains (ε_{mech}) induced in the sample by the thermal cycles as shown in Eq. 3.

$$\varepsilon_{mech} = \varepsilon_{total} - \varepsilon_{therm} \qquad \text{Eq. 3}$$

In spite of the total strains measured at the point P1 presents mostly positive values, the centre of the disk is under compression. The decomposition of the total strain, into thermal and mechanical strains, allows us to better understand the strains developed at point P1 during the thermal cycles (cf. Figure 7).

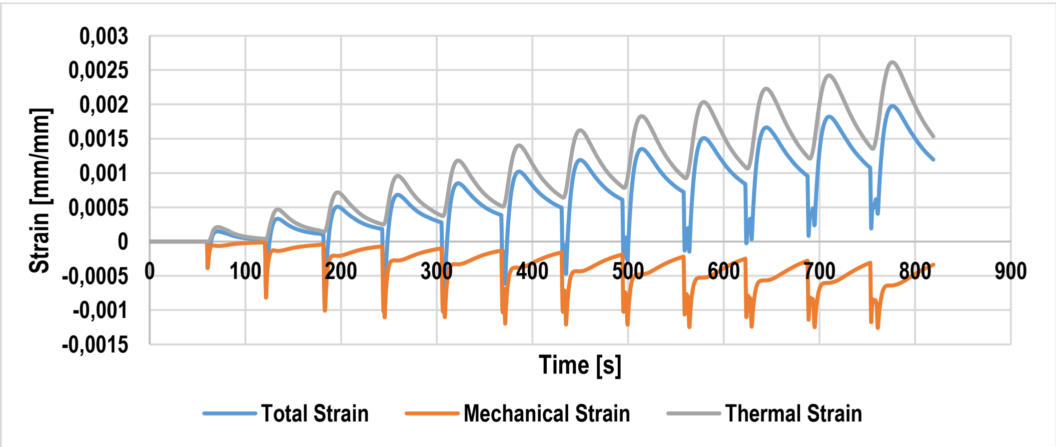

Figure 7: Decomposed strains developed in the alumina spinel sample at point P1 (from numerical model)

3.3 OUT-OF-PLANE DISPLACEMENTS

The use of stereovision allows the determination of the out-of-plane displacements. Figure 8 presents the comparison of the out-of-plane displacements determined experimentally and numerical at point P1.

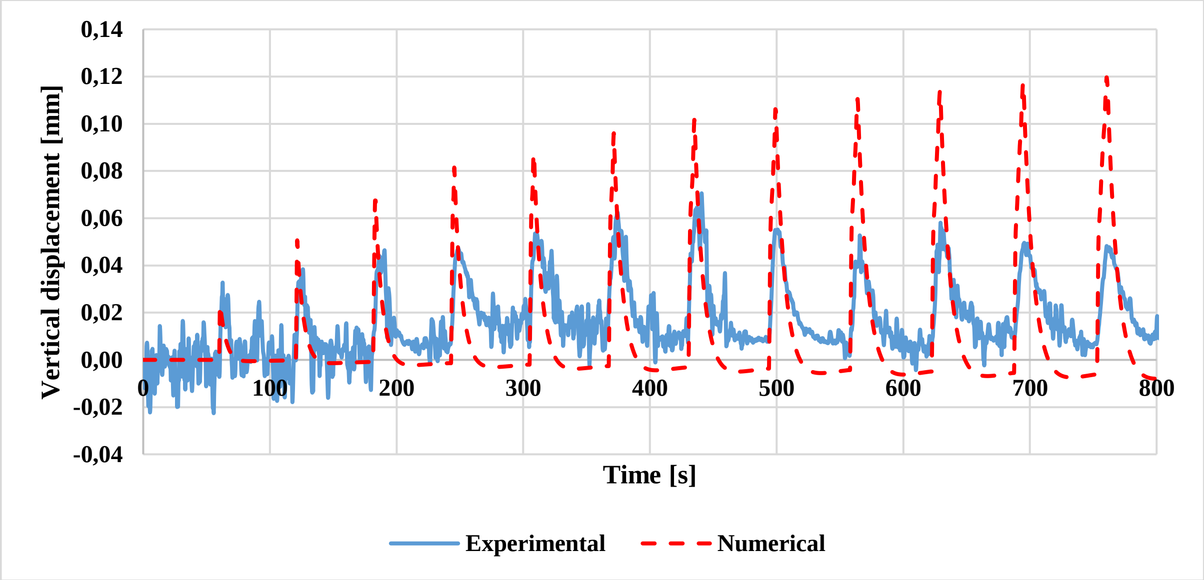

Figure 8: Comparison of out-of-plane displacement evolution for the central point at the bottom surface (point P1).

The thermal gradient, through the thickness of the sample, leads to a thermal bowing, therefore, it is possible to identify an upward displacement in the centre of the sample (point P1). In spite of small measured displacements (from 0.02 mm for the first cycle to 0.12 mm for the last one), a quite good correlation was found between the experimental data and the numerical model, especially for the three first cycles. For example for the second heating (at 120 s), the maximum displacement measured by the stereovision system was 0.04 mm and the maximum displacement calculated by the numerical model was 0.045 mm. After the fourth heating cycle, increasing differences between experimental values at pic and values predicted by simulation could be explained by the emergence of important cracks within the sample after 250 s (presented in next part and not taken into account within the FEM model).

3.4 FRACTURE BEHAVIOUR

The analysis of the fracture behaviour of the alumina spinel disk is presented in this section. As previously mentioned, the thermal gradient, between the centre and the borders of the disk, leads to compressive stress at the centre and tensile stress at the borders of the sample, in the circumferential direction. The successive heating laser pulses of increasing duration, lead to a progressive increase of circumferential tensile stress at the border of the disk. When this circumferential tensile stress reaches the tensile strength of the alumina spinel material, a crack can start at the border and then can progress toward the centre of the disk. Sample pictures with highlighted crack path, detected by the 2P-DIC method, are presented on Figure 9.

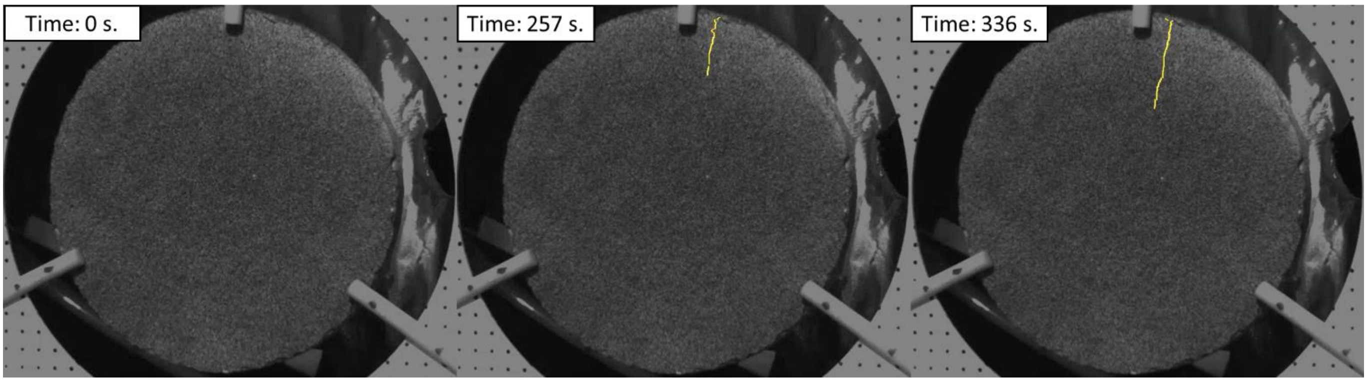

Figure 9: Pictures with crack path (detected by 2P-DIC method) observed on alumina spinel sample: a) without fracture; b) right after crack initiation (at 257 s); c) one heating cycle after crack initiation (336 s).

Figure 10: Crack opening near the sample border (bottom surface) and developed stresses at the border (top face and bottom face). presents the crack opening (measured by relative displacement of two little subsets located on both sides of the crack initiation area) and compares it to the developed stresses in the border of the sample, predicted by the numerical simulation. It should be noted that tensile stress at top face is higher than at the bottom face. Consequently, the crack is expected to start at the edge of the top face and then propagates to the bottom face. These predicted numerical stress values should be compared with experimental values of strength for investigated alumina-spinel brick, but these experimental values of strength can significantly varies depending on considered mechanical test for tensile strength valuation: typically 1.6 MPa measured in pure tension, 3.4 MPa measured by Brazilian test and 5.2 MPa evaluated from wedge splitting test. Considering an assumed local tensile stress threshold (an average value) that could be taken in account for crack onset, it is possible to identify a good correlation between local tensile stress values and the moment in which the crack really starts (observed by DIC).

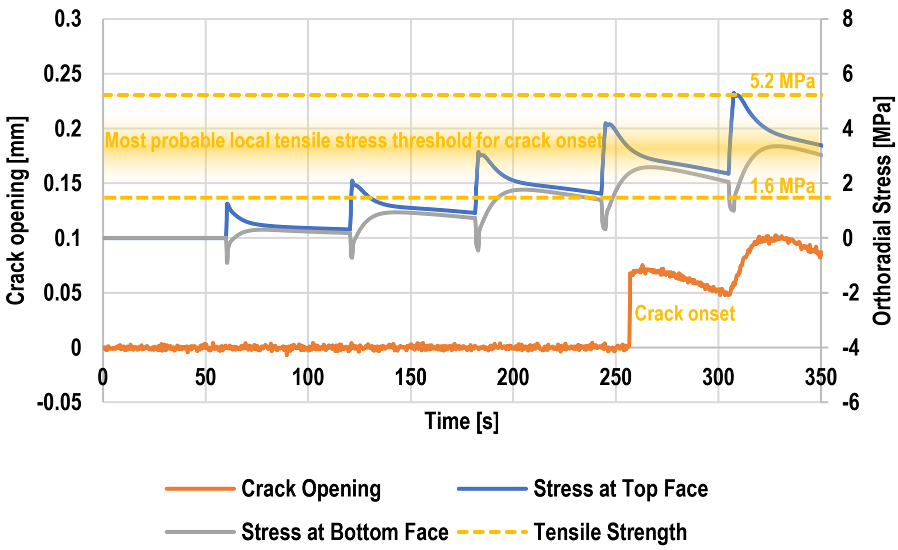

Figure 10: Crack opening near the sample border (bottom surface) and developed stresses at the border (top face and bottom face).

4 Conclusion

This document summarizes the characterization of refractory materials under cyclic thermal gradient at sample scale (brick). A dedicated device (ATHORNA for Advanced measurements for in-situ Thermomechanical monitORing of large sample uNder thermal gradient) has been developed to monitor the behaviour of a cylindrical disk subjected to a concentrated heat flux. A CO_2 laser allows the modulation of heating power and adjustment of cycles applied at the top face of the sample. An infrared camera allows the measurement of the temperature fields at the bottom face of the sample. A stereo-vision cameras and the digital image correlation allow the measurement of displacements and strains. Application of DIC with two subsets located on both sides of crack is useful to determine crack opening (detection of crack initiation time) and to compare this crack initiation time with the time for which predicted numerical stress can reach material strength.

In order to demonstrate the potential of the developed ATHORNA device, an alumina spinel disk was subjected to twelve thermal cycles and in parallel, a numerical model was developed to simulate the performed test. As demonstrated, the numerical model has been validated against the experimental results with good accuracy.

The temperature fields and the thermal gradients developed within the sample were presented in section 3.1. As described, there are two thermal gradients in the sample: *i*) through the thickness of the sample and *ii*) between the centre and the borders. The strain fields were described in section 3.2. The out-of-plane displacement caused by the thermal bowing of the sample was shown in section 3.3. The measured temperatures, strains and displacement are in good agreement with the predictions of the numerical FEM model.

The fracture behaviour of the sample was described in section 3.4. Considering most probable local tensile strength, it has been possible to identify a good correlation between local tensile stress values evaluated by FEM modelling and the observation of crack onset by DIC and 2P-DIC.

The present deliverable present only few results that demonstrate the pertinence of ATHORNA device to validate complex numerical FEM thermomechanical modelling at the intermediate scale of a cylindrical disc (10 to 15 cm in diameter) but that could be further used for larger industrial scale. More complete results will be presented in scientific papers that will be available soon.

5 References

[1] R. Kaczmarek, J-C. Dupré, P. Doumalin, IO. Pop, L. Teixeira, J. Gillibert, E. Blond, M.Huger, 'Thermomechanical behaviour of an alumina spinel refractory for steel ladle applications', *Proceedings* of *UNITECR congress*, 2019, Yokohama, Japan, pp. 2-5.

[2] J-C. Dupré, P. Doumalin, Y. Belrhiti, I. Khlifi, O. Pop, M. Huger, 'Detection of cracks in refractory materials by an enhanced digital image correlation technique', Journal of Materials Science, 2018, vol. 53, no. 2, pp. 977-993, doi: 10.1007/s10853-017-1550-3.

[3] Dassault Systems Simulia Corporation, *Abaqus User Manual*. USA, 2010.

[4] A. Gasser, K. Terny-Rebeyrotte, P. Boisse, 'Modelling of joint effects on refractory lining behaviour', *Proc. Inst. Mech. Eng. Part J. Mater. Des. Appl.*, 2004, vol. 218, no. 1, pp. 19-28, doi: 10.1177/146442070421800103.

[5] M. Ali, T. Sayet, A. Gasser, E. Blond, 'Transient Thermo-Mechanical Analysis of Steel Ladle Refractory Linings Using Mechanical Homogenization Approach', *Ceramics*, 2020, vol. 3, no. 2, Art. no. 2, doi: 10.3390/ceramics3020016.